ความแม่นยำของการตรวจวินิจฉัยมะเร็งต่อมลูกหมากด้วยเครื่องตรวจคลื่นสนามแม่เหล็กไฟฟ้าด้วยวิธีการหลายพารามิเตอร์

ชลิดา อภินิเวศ*, ชยานนท์ ชินพรเจริญพงษ์, กุลญาดา สมทรัพย์, วัลลภ เหล่าไพบูลย์

ภาควิชารังสีวิทยา คณะแพทยศาสตร์ มหาวิทยาลัยขอนแก่น จังหวัดขอนแก่น

Accuracy of Multi-parametric Magnetic Resonance Imaging for Diagnosis of Prostate Cancer

Chalida Aphinives*, Chayanon Chinporncharoenpong, Kulyada Somsap, Vallop Laopaiboon.

Department of Radiology, Faculty of Medicine, Khon Kaen University, Khon Kaen, 40002, Thailand.

วัตถุประสงค์: เพื่อศึกษาความแม่นยำของการตรวจวินิจฉัยมะเร็งต่อมลูกหมากด้วยเครื่องตรวจคลื่นสนามแม่เหล็กไฟฟ้าด้วยวิธีการหลายพารามิเตอร์

วิธีการศึกษา: เป็นการศึกษาย้อนหลังในผู้ป่วยที่ได้รับการตรวจด้วยเครื่องตรวจคลื่นสนามแม่เหล็กไฟฟ้า ร่วมกับการเจาะตรวจชิ้นเนื้อทางพยาธิวิทยาผ่านเครื่องตรวจคลื่นเสียงทางทวารหนัก ระหว่างเดือน กรกฎาคม 2555 ถึง สิงหาคม 2557 ภาพการตรวจด้วยคลื่นสนามแม่เหล็กไฟฟ้าประกอบด้วยหลายพารามิเตอร์ ได้แก่ ADC, DCE-MRI, Cho/cit ratio และ (Cho+creat)/cit ratio แล้วประเมินความแม่นยำในการตรวจวินิจฉัยโดยอาศัย AUC

ผลการศึกษา: การศึกษานี้ครอบคลุม 36 รอยโรคจากผู้ป่วย 28 ราย รอยโรคที่เป็นมะเร็งใน peripheral zone ให้ค่า ADC ต่ำกว่ารอยโรคที่ไม่ใช่มะเร็งอย่างมีนัยสำคัญ (p < 0.01) หากรอยโรคนั้นมีขนาดตั้งแต่ 1 ซม. ขึ้นไป จะให้ค่า (Cho+creat)/cit ratio สูงกว่าอย่างมีนัยสำคัญ พารามิเตอร์ ADC มีความจำเพาะสูงถึงร้อยละ 87.5 ความแม่นยำร้อยละ 77.8 และ AUC 0.68 เช่นเดียวกันกับ พารามิเตอร์ DCE-MRI มีความจำเพาะสูงถึงร้อยละ 91.7 ความแม่นยำร้อยละ 83.3 และ AUC 0.78 พารามิเตอร์ Cho/cit ratio มีความจำเพาะสูงถึง ร้อยละ 91.7 แต่ความแม่นยำต่ำเพียงร้อยละ 54.2 เมื่อนำพารามิเตอร์ DCE-MRI มาร่วมกับ Cho/cit ratio จะให้ค่า AUC สูงที่สุดที่ 0.85 และมีความแม่นยำถึงร้อยละ 83.3 อย่างไรก็ตามการนำพารามิเตอร์ทั้งสามมาใช้ร่วมกัน กลับไม่ได้เพิ่มประสิทธิภาพอย่างมีนัยสำคัญ

สรุป: การตรวจด้วย DCE-MRI ร่วมกับ ADC มีความแม่นยำในการตรวจวินิจฉัยมะเร็งต่อมลูกหมาก สูงกว่าการตรวจด้วย MRS

Objective: To assess the diagnostic accuracy of magnetic resonance imaging (MRI) for prostate cancer with multiple parameters.

Methods: Patients who underwent both MRI and transrectal ultrasound-guided biopsy from July 2012 to August 2014, were reviewed retrospectively. Multiple parameters were assessed to determine the accuracy of MRI for prostate cancer; the apparent diffusion coefficient (ADC), dynamic contrast enhanced MRI (DCE-MRI), and the Cho/cit and (Cho+creat)/cit ratios. The areas under the receiver operating characteristic curves (AUC) were used to evaluate the diagnostic accuracy of metabolic ratios.

Results: Thirty-six lesions from 28 patients were analyzed. Malignant lesions at the peripheral zone showed significantly lower ADCs than benign lesions (p < 0.01). If lesion size was 1 cm or larger, the (Cho+creat)/cit ratio was significantly higher (p < 0.01). The ADCs had a high specificity of 87.5%, an accuracy of 77.8%, and AUC of 0.68. DCE-MRI had high specificity of 91.7%, accuracy of 83.3%, and an AUC 0.78. The Cho/cit ratios showed a high sensitivity of 91.7%, but low specificity of 54.2%. The greatest AUC was 0.85 when the DCE-MRI was combined with the Cho/cit ratio, giving an accuracy of 83.3%. No significant improvement was established, however, when all 3 parameters were combined together.

Conclusion: DCE-MRI and ADC had greater diagnostic accuracy than MR spectroscopy (MRS). Combined

*Corresponding author :   Chalida Aphinives; 123 Group 16, Mittraparp Rd, Muang, Khon Kaen province, 40002, Thailand; Tel: 0-4336-3614. E-mail: chalida.aphinives@gmail.com

parameters improved specificity for prostate cancer lesions.

Introduction

Prostate cancer is one of the most common cancers found in men.[1] The roles of Magnetic Resonance Imaging (MRI) in the evaluation of prostate cancer are detection and staging of cancer. Multiparametric MRI is recommended in the guidelines by the European Society of Urogenital Radiology (ESUR) 2019 which consists of high resolution T2-weighted imaging (T2WI), diffusion weighted imaging (DWI), dynamic contrast enhanced MRI (DCE-MRI), and MR spectroscopy (MRS).[2] The additional MRS increases acquisition time of approximately 12 minutes and cost, however, while DCE-MRI requires Gadolinium administration that may harmful in patients with renal disease and increases the risk of developing nephrogenic systemic fibrosis. The purpose of this study was to determine diagnostic accuracy of each parameter and comparing results among parameters of multiparametric MRI in detecting prostate cancer.

Materials and Methods

This retrospective study was conducted under approval by the institute Human Research Ethics Committee and with the Helsinki Declaration of 1975, as revised in 2000. Medical records of 31 patients who underwent MRI of prostate glands and transrectal ultrasound-guided biopsy from July 2012 to August 2014, were retrospectively reviewed. Three cases were excluded because of no DCE-MRI. All 28 remaining cases underwent transrectal ultrasound-guided biopsy within 3 months after MRI. No patients had a previous history of cancer, pelvic radiation or chemotherapy.

MRI studies were performed on Aera (1.5T Siemens) and Achieva (3T Philips). Conventional T2-weighted turbo spin echo imaged (TSE; TR/ TE, 3000/100 ; matrix size, 256x512; slice thickness, 2.5-3 mm; field of view, 14 cm^2; total acquisition time 3 minutes) were obtained in three orthogonal planes.

Echo-planar diffusion-weighted images (TR/TE, 2500/57.2; matrix size, 108x164; field of view, 240x260 mm; b values of 0, 800, and 1000 s/mm2; acquisition time, 4 minutes) were obtained transverse to the prostate. The phase-encoding gradient was left to right to minimize motion artifacts in the prostate. ADC maps were generated using the manufacturing software.

A two-dimensional chemical shift imaging (CSI) was performed over a single slice transverse to the prostate, using the thickness of 12 mm and a 9-16 grid (voxel size 12x12x12 mm^3). The slice was selected by the same offsets as a T2-weighted slice that showed a focal low-signal-intensity abnormality within a prostate that suspected for lesion. Signal collection was restricted to voxels over the prostate using the point-resolved spectroscopy (PRESS) localization technique (TR/TE, 1400/140). Data acquisition took 9-12 minutes. The spectroscopy data were voxel-shifted to align the CSI data set with the PRESS box and analysis using a basis set containing metabolite spectra from choline, creatine, and citrate.

An external pelvic phased-array coil was used to acquire axial T1-weighted (TSE; TR/TE, 555/8) and T2-weighted (TSE; TR/effective TE, 1250/70) images through the pelvis.

A three-dimensional fast low-angle shot sequence was used to perform DCE MR imaging. After four baseline acquisitions, gadobutrol (gadolinium chelate; Gadovist) was administered as a bolus injection of 0.1 mmol/kg of body weight at a rate of 2-4 mL/sec, contrast enhanced images were acquired with a temporal resolution of 9 seconds for 5 minutes.

The lesions were selected based on T2WI in the three orthogonal planes in peripheral zone and central gland by two radiologists, who had 3 and 6 years' experiences in interpreting prostate MRI. Matched and consensused data between two radiologists were used for statistical analysis.

Size of lesion was measured on transverse T2WI. ROIs for apparent diffusion coefficient (ADC) value

were drawn involving at least fifty percent of lesions to measured ADC value. Three ADC values were obtained for each lesion and used average ADC value for data analysis. DCE-MRI was evaluated by qualitative approach and semiquantitative approach[2]. The qualitative, or visual, analysis was based on the general assumption that malignant tumors will show early rapid enhancement and relatively rapid decline compared with the normal tissues. This approach was subjective and the least standardized. The semiquantitative approach, or curveology, is calculated curve parameter that showed slope, peak enhancement, wash-in and wash-out curve shaped. Dynamic curve types were categorized in 3 types: type 1, persistent increase; type 2, plateau; and type 3, decline. Type 3 was the most suspicious for malignancy[2] and interpreted as positive result in this study. For MRS, ROIs were correlated with T2WI then CSI slice were overlaid onto the CSI grid. Voxels were included in the data analysis if more than 70% voxel was within the lesion. Cho/cit ratios and (Cho+creat)/cit ratios were collected for each selected voxel. For paired parameter, diagnosis of malignancy was given when both parameters were positive.

Analysis of selected lesions correlated with pathological reports from transrectal ultrasound-guided biopsy was diagnosed as malignant lesion when positive tissue for carcinoma was on the same side of prostate as the selected lesion and not interfered by another selected lesion. Transrectal ultrasound-guided biopsy was a gold standard in this study.

Statistical analysis was performed using excel XLSTAT software (Version 2014.6.04 for Windows). The ADC showed normal distribution by means of Jarque-Bera test, two sample t-test was used. Mann-Whitney test were used for the Cho/cit and (Cho+creat)/cit ratios that not followed normal distribution. Sensitivities and specificities in detection of malignancy with an individual parameter alone were calculated. Area under curve (AUC) of the receiver operating characteristics curve (ROC) was used to quantify the power of ADC, Cho/cit ratio, (Cho+creat)/cit ratio and dynamic curve type. Correlations between pairs of tissue parameters, patient age, prostate-specific antigen (PSA) level, and size of tumor were examined with Pearson's correlation coefficient. A p value of less than 0.01 was considered statistically significant difference.

For pairs of parameters and multiparameter, diagnostic analysis was used for sensitivity, specificity, positive predictive value (PPV), negative predictive value (NPV) and accuracy. The cut off points for positive data of ADC, Cho/cit, and (Cho+creat)/cit ratios were analyzed from ROC curve. The combination of multi-parameter was analyzed with logistic regression and ROC curve to calculate AUC.

Results

The patient mean age was 67 years old (range 56-82 years). The median of PSA was 10.1 ng/mL (range 3.4-100 ng/mL), which differed significantly between benign and malignant lesions (9.9 VS 24.1, $p < 0.05$) as shown in Table 1.

The ADC was significantly lower in malignant lesions compared with benign lesions in the peripheral zone ($p < 0.05$). There were also significant differences of Cho/cit and (Cho-creat)/cit ratios between benign and malignant lesions in the peripheral zone, however, this was limited only to lesions larger than 1 cm (Table 2).

Ten of 36 lesions showed dynamic curve type 3; 8 lesions were confirmed as malignant lesions while the remaining 2 lesions were benign (Table 3). DCE-MRI showed a sensitivity of 66.7%, specificity of 91.7% and accuracy of 83.3%, PPV of 80.0%, NPV of 84.6%. The AOC curves gave a cutoff value at 0.96 s/mm2 which had a sensitivity of 58.3%, specificity of 87.5% and accuracy of 77.8% (Table 4).

ADC and DCE-MRI alone had high specificities of 87.5% and 91.7%, but low sensitivities of 58.3% and 66.7%. The Cho/cit gave a higher sensitivity of 91.7%, but a lower specificity of 54.2% (Figure 1). The accuracies for each of the parameters were 77.8% for ADC, 83.3% for DCE-MRI, 66.7% for Cho/cit ratios, and 61.1% for (Cho+creat)/cit ratios. The paired combinations of ADC with MRS and DCE-MRI with MRS showed high specificity but low sensitivity. The combination of ADC and DCE-MRI showed the greatest specificity of 91.7% (Figure 2). The multi-parameters of ADC, DCE-MRI and MRS showed a fair specificity but was lower than any paired parameters with no significant difference in sensitivity (Table 4).

Discussion

Several studies showed various sensitivities and specificities in use for each technique alone and higher diagnostic accuracy when combined with at

Table 1 Characteristics of Study

Characteristic	Value
Age (year)	
Mean ± SD	67 ± 7.5
Range	56-82
PSA (ng/mL)	
Median	
Benign	10
Malignancy	9.9
Range	24.1
Quartiles	3.4-100.0
Pathological diagnosis (patient)	6.9,26.6
Adenocarcinoma	
Nodular hyperplasia	11
Prostatitis	7
PIN grade I	7
Negative for malignancy	1
Total	2
Location (lesion)	28
Central gland	
Benign	19
Malignancy	17 (47%)
Peripheral zone	2 (5.5%)
Benign	17
Malignancy	7 (19%)
Total	10 (27.8%)
Size (mm)	36
Mean ± SD	13.6 ± 6.9
Range	5-34
Size ≥ 1 cm	25

Figure 1 ROC curves

Figure 2 ROC curves for combinations
*MRS1 = Cho/cit ratio, MRS2 = (Cho+creat)/cit ratio

least 2 functional techniques. The comparisons of accuracy among ADC, DCE-MRI, MRS, paired parameters, and multi-parameters had an influence for decisions of which modalities were more suitable.[3-7] This current study showed that malignant lesions exhibited lower ADCs in all sized lesions within the peripheral zone, especially in the lesions which were larger than 1 cm. Liu, et al8 reported the use of ADC for central gland lesions. The study herein did not include enough central gland malignant lesions, so it
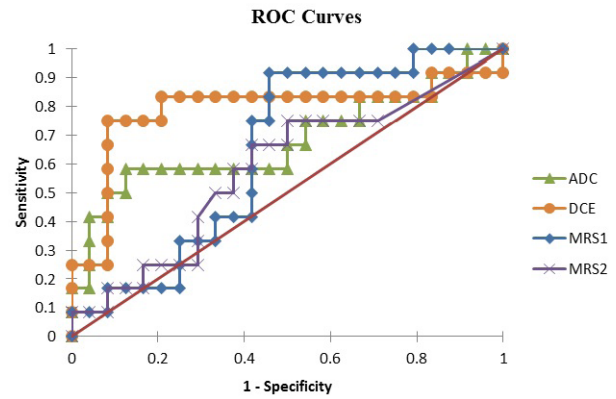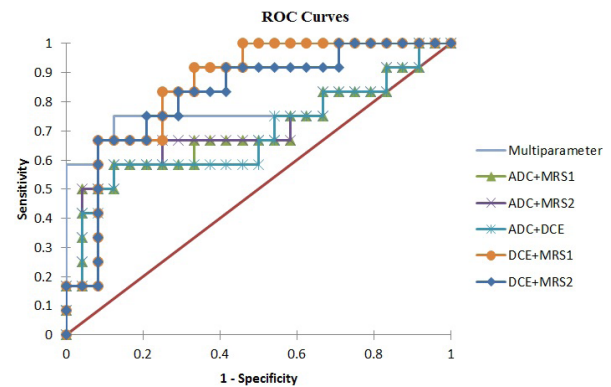
was not possible to analyze this point. The study showed a cutoff point at $0.95 \times 10\text{-}3 \text{ mm}^2/\text{s}$ which correlated well with another study (range $0.93 – 1.38 \times 10^{-3} \text{ mm}^2/\text{s}$).[9]

In this study, DCE-MRI was interpreted by dynamic curves which showed a good specificity of 91.7%; the same as other studies.[10, 11] The accuracies and AUCs of DCE-MRI were also greater than other parameters; a combination of DCE-MRI with ADC or MRS did improve the specificity and AUC compared to one parameter alone.

Several studies[12-16] mentioned MRS for improving the accuracy of prostate cancer detection. An increase of Cho/cit or (Cho+creat)/cit ratios were most reliable in the peripheral zone. In the present study, significant increases of metabolite ratios in the peripheral zone were found only in lesions larger than 1 cm (p < 0.01). Metabolic signals from small or infiltrative malignant lesions might be obscured by strong signals from surrounding normal tissue in voxels. This study showed that the Cho/cit ratio alone gave a high sensitivity of 91.7%, but both Cho/cit and (Cho+creat)/cit ratios had low specificities without significant differences when lesions larger than 1 cm. were

Table 2 Functional parameters of benign and malignant lesions

Parameter	ADC (x10⁻³ s/mm²)	Cho/cit Ratio	(Cho+creat)/cit ratio
All lesions			
Malignant	0.95 ± 0.55	9.96 ± 24.0	10.45 ± 26.1
Benign	1.29 ± 0.38	4.11 ± 10.1	3.47 ± 8.5
Malignant vs benign		p = 0.17	p = 0.42
Central gland lesion			
Malignant	0.99 ± 0.65	1.91 ± 1.1	0.92 ± 1.3
Benign	1.19 ± 0.37	2.90 ± 6.8	2.64 ± 6.0
Malignant vs benign	p = 0.74	p = 0.46	p = 0.64
Peripheral zone lesion			
Malignant	0.95 ± 0.57	11.57 ± 26.2	12.36 ± 28.4
Benign	1.54 ± 0.30	7.05 ± 15.9	5.47 ± 13.2
Malignant vs benign	p = 0.01*	p = 0.41	p = 0.24
Lesion size ≥ 1 cm			
Malignant	0.73 ± 0.41	13.01 ± 27.4	13.82 ± 29.8
Benign	1.33 ± 0.37	3.23 ± 6.9	0.69 ± 6.2
Malignant vs benign	p < 0.01*	p = 0.17	p = 0.18
Central gland lesion			
Malignant	0.98 ± 0.29	1.94 ± 1.1	0.93 ± 1.3
Benign	1.28 ± 0.4	4.29 ± 8.2	3.8 ± 7.2
Malignant vs benign	p = 0.64	p = 0.9	p = 0.43
Peripheral zone lesion			
Malignant	0.66 ± 0.36	16.12 ± 30.7	17.5 ± 33.3
Benign	1.46 ± 0.29	0.88 ± 1.4	0.22 ± 0.4
Malignant vs benign	p < 0.01*	p = 0.05*	p < 0.01*

Table 3 Dynamic Contrast-Enhanced Curve

Characteristic	Value
All lesion	36
Curve type 2	
Malignant	4 (15.3 %)
Benign	22 (84 %)
Total	26
Curve type 3	
Malignant	8 (80 %)
Benign	2 (20 %)
Total	10

analyzed. MRS combined with ADC or DCE-MRI increased specificity, sensitivity and accuracy. For ROC curve analysis, cutoff points for Cho/cit and (Cho+creat)/cit ratios of all lesions were 0.79 and 1.10.

The study showed that DCE-MRI gave greater specificity of 91.7%, while Cho/cit ratios had better sensitivity of 91.7%. Moreover DCE-MRI was clearly significantly superior in accuracy of 83.3% and AUC, when compared with both Cho/cit and (Cho+creat)/cit ratios. In lesions larger than 1 cm, DCE-MRI still had a better specificity of 93.3%, an accuracy of 85.7%, and in the AUC. On the other hand, Cho/cit and (Cho+creat)/cit ratios showed increases in sensitivity of 100% and 77.8%, but still had low specificities of

Table 4 Sensitivity, Specificity and Accuracy of Parameters

Parameter	Cut off	AUC	Sensitivity (%) [95% CI]	Specificity (%) [95% CI]	Accuracy (%)
All lesions					
ADC	0.95 x10-3 s/mm^2	0.68	58.3 [27.7, 84.8]	87.5 [67.6, 97.3]	77.8
DCE-MRI	-	0.79	66.7 [38.8, 86.2]	91.7 [72.8, 98.7]	83.3
Cho/cit ratio	0.79	0.64	91.7 [59.8, 99.6]	54.2 [33.2, 73.8]	66.7
(Cho+creat)/cit ratio	1.1	0.58	66.7 [35.4, 88.7]	58.3 [36.9, 77.2]	61.1
Combined parameters					
ADC + DCE-MRI	-	0.68	50.0 [25.5, 74.5]	91.7 [72.8, 98.7]	77.8
ADC + MRS 1	-	0.7	50.0 [25.5, 74.5]	95.8 [77.8, 100]	80.6
ADC + MRS 2	-	0.71	50.0 [25.5, 74.5]	95.8 [77.8, 100]	80.6
DCE-MRI + MRS 1	-	0.85	66.7 [38.8, 86.2]	91.7 [72.8, 98.7]	83.3
DCE-MRI + MRS 2	-	0.85	41.7 [19.4, 68.1]	91.7 [72.8, 98.7]	75
ADC + DCE-MRI +MRS 1	-	0.78	66.7 [38.8.,86.2]	91.7 [72.8, 98.7]	83.3
ADC + DCE-MRI +MRS 2	-	0.78	66.7 [38.8, 86.2]	91.7 [72.8, 98.7]	83.3
Lesion size ≥ 1 cm					
ADC	0.95 x10-3 s/mm^2	0.85	77.8 [40.0, 97.2]	93.8 [69.8, 99.8]	88
DCE-MRI	-	0.82	66.7 [29.6, 90.4]	93.3 [67.8, 100]	85.7
Cho/cit ratio	0.74	0.67	100 [65.0, 100]	50.0 [28.1, 71.9]	68
(Cho+creat)/cit ratio	1.15	0.67	77.8 [44.1, 94.3]	62.5 [38.8, 81.5]	68

Note: MRS 1= Cho/Cit ratio, MRS 2 = (Cho+creat)/cit ratio, AUC = area under curve

50% and 62.5%. These results that differed from Riches et al[5] might be due to the differences in methods of analysis of quantitative methods VS semi-qualitative methods.

This study also showed that any paired parameter combination increased specificity but no significant differences were found between each of the paired parameters (Table 4). The best diagnostic paired parameter was DCE-MRI with the Cho/cit ratio which had a sensitivity of 66.7%, specificity of 91.7%, an accuracy of 83.35%, and AUC of 0.85. However, this retrospective study contained small amount of subjects, so prospective study with more subjects should further conducted.

Conclusion

In conclusion, DCE-MRI and ADC had far greater specificity and accuracy than MRS while Cho/cit ratio had greater sensitivity. The combination of paired parameters improved specificity and accuracy. The adding of a 3rd parameter, however, did not improve the accuracy for diagnosis of prostate cancer.

References

1. Siegel RL, Miller KD, Jemal A. Cancer Statistics, 2017. CA Cancer J Clin 2017; 67(1): 7–30.

2. Barentsz JO, Richenberg J, Clements R, Choyke P, Verma S, Villeirs G, et al. ESUR prostate MR guidelines 2012. Eur Radiol 2012; 22(4): 746–757.

3. de Rooij M, Hamoen EHJ, Fütterer JJ, Barentsz JO, Rovers MM. Accuracy of multiparametric MRI for prostate cancer detection: a meta-analysis. AJR Am J Roentgenol 2014; 202(2): 343–351.

4. Reinsberg SA, Payne GS, Riches SF, Ashley S, Brewster JM, Morgan VA, et al. Combined use of diffusion-weighted MRI and 1H MR spectroscopy to increase accuracy in prostate cancer detection. AJR Am J Roentgenol 2007; 188(1): 91–98.

5. Riches SF, Payne GS, Morgan VA, Sandhu S, Fisher C, Germuska M, et al. MRI in the detection of prostate cancer: combined apparent diffusion coefficient, metabolite ratio, and vascular parameters. AJR Am J Roentgenol 2009; 193(6): 1583–1591.

6   Fütterer JJ. Multiparametric MRI in the Detection of Clinically Significant Prostate Cancer. Korean J Radiol. 2017; 18(4): 597–606.

7. Gao P, Shi C, Zhao L, Zhou Q, Luo L. Differential diagnosis of prostate cancer and noncancerous tissue in the peripheral zone and central gland using the quantitative parameters of DCE-MRI: A meta-analysis. Medicine (Baltimore). 2016; 95(52): e5715.

8. Liu X, Zhou L, Peng W, Wang C, Wang H. Differentiation of central gland prostate cancer from benign prostatic hyperplasia using monoexponential and biexponential diffusion-weighted imaging. Magn Reson Imaging 2013; 31(8): 1318–1324.

9. Woodfield CA, Tung GA, Grand DJ, Pezzullo JA, Machan JT, Renzulli JF. Diffusion-weighted MRI of peripheral zone prostate cancer: comparison of tumor apparent diffusion coefficient with Gleason score and percentage of tumor on core biopsy. AJR Am J Roentgenol 2010; 194(4): W316-322.

10. Verma S, Turkbey B, Muradyan N, Rajesh A, Cornud F, Haider MA, et al. Overview of dynamic contrast-enhanced MRI in prostate cancer diagnosis and management. AJR Am J Roentgenol 2012; 198(6): 1277–1288.

11. Casciani E, Polettini E, Bertini L, Emiliozzi P, Amini M, Pansadoro V, et al. Prostate cancer: evaluation with endorectal MR imaging and three-dimensional proton MR spectroscopic imaging. Radiol Med 2004; 108(5–6): 530–541.

12. Panebianco V, Sciarra A, Ciccariello M, Lisi D, Bernardo S, Cattarino S, et al. Role of magnetic resonance spectroscopic imaging ([1H]MRSI) and dynamic contrast-enhanced MRI (DCE-MRI) in identifying prostate cancer foci in patients with negative biopsy and high levels of prostate-specific antigen (PSA). Radiol Med 2010; 115(8): 1314–1329.

13. Hasumi M, Suzuki K, Oya N, Ito K, Kurokawa K, Fukabori Y, et al. MR spectroscopy as a reliable diagnostic tool for localization of prostate cancer. Anticancer Res 2002; 22(2B): 1205–1208.

14. Bellomo G, Marcocci F, Bianchini D, Mezzenga E, D'Errico V, Menghi E, et al. MR Spectroscopy in Prostate Cancer: New Algorithms to Optimize Metabolite Quantification. PLoS ONE 2016; 11(11): e0165730.

15. Prostate imaging – Reporting and data system (PI-RADS) version 2.1 2019 American college of radiology. [https://www.acr.org/-/media/ACR/Files/RADS/Pi-RADS/PI-RADS-V2-1.pdf?la=en]

16. Rezaeian A, Tahmasebi BMJ, Chegeni N, Sarkarian M, Hanafi MG, Akbarizadeh G. Signal intensity of high B-value diffusion-weighted imaging for the detection of prostate cancer. J Biomed Phys Eng 2019; 9(4): 453-458.

SMJ